Journal of Computational Physics 462 (2022) 111256

Contents lists available at ScienceDirect

Journal of Computational Physics

www.elsevier.com/locate/jcp

Short note

An appropriate numerical dissipation for SLAU2 towards shock-stable compressible multiphase flow simulations

Junya Aono *, Keiichi Kitamura

Yokohama National University, 79-5 Tokiwadai, Hodogaya-ku, Yokohama, Kanagawa 240-8501, Japan

ARTICLE INFO

Article history:
Received 15 August 2020
Received in revised form 5 March 2021
Accepted 24 April 2022
Available online 29 April 2022

Keywords:
AUSM-family
Numerical dissipation
Multiphase flow
Material interface

ABSTRACT

This paper proposes a novel method for the computation of compressible multiphase flows under the assumption of pressure equilibrium based on a 6-equation model and the AUSM (Advection Upstream Splitting Method) family. In this study, we introduce a new numerical pressure flux dissipation term based on the relative velocities in the gas and liquid phases to develop an analogous carbuncle-suppression mechanism that is applicable to gas dynamics. We also propose a mass flux dissipation term based on the pressure ratio at the gas-liquid interface and incorporate both terms into SLAU2, an AUSM-family scheme, to achieve robustness against shock anomalies.

1. Introduction

Multiphase flows arise in various fields that entail complicated phenomena such as the breakup of water droplets, and their phase changes under cavitation, evaporation, boiling, and condensation. The flow inside a liquid rocket engine is an example of a multiphase flow comprising both gaseous and liquid phases, where liquid oxygen initially breaks up and evaporates and is mixed with fuel in a combustion chamber. Then, both the liquid oxygen and the fuel undergo combustion, accompanied by possible instabilities such as resonance in the engine due to fluctuations in the rate of heat release [1]. To address such problems, simultaneous solutions of sound waves and compressible flows are required; hence, compressible multiphase flow computation has become an important topic of research in this field. Multiphase flow simulations have been extensively studied by many researchers. Multiphase flow simulations are classified into two categories: those that follow the Eulerian-Lagrangian approach [2] and those based on the Eulerian-Eulerian approach. In the Eulerian-Lagrange approach, the liquid phase is expressed by particles, and, as a result, gas-liquid interfaces and primary atomization cannot be treated.

We now review a compressible multiphase flow method based on a 6-equation model, proposed by Liou [3], incorporating an interfacial pressure term (two-fluid model), proposed by Stuhmiller [4], with a pressure equilibrium assumption. However, it has been reported to be incapable of continuing calculations without switching to the exact Riemann (Godunov) solver [5] following strong shocks or volume fraction discontinuities owing to induced stability and robustness issues [6]. Further, the exact Riemann (Godunov) solver is known to incur high computational costs and exhibit a particular instability called the carbuncle phenomenon in the analysis of shock waves [7]. It has not yet been possible to completely eliminate the carbuncle phenomenon, but certain Advection Upstream Splitting Method (AUSM) schemes have been reported to be more stable than the Roe flux or the exact Riemann solver [8] in this context. Thus, Chang and Liou hybridized Godunov

* Corresponding author.
E-mail address: aono-junya-py@ynu.jp (J. Aono).

https://doi.org/10.1016/j.jcp.2022.111256

(at the gas-liquid interface) using AUSM$^+$-up (elsewhere) to propose an all-speed, shock-robust multiphase flow solver [9]. Kitamura [6] extended this work and proposed the Godunov-SLAU2 (G-SLAU2), a parameter-free, all-speed, shock-robust multiphase flow solver. Five years later, Pandare [10] developed AUSM$^+$-upf (belonging to the AUSM-family), which introduced appropriate numerical dissipation to AUSM$^+$-up proposed by Liou [11]. Without using the Godunov solver, it executed stable and robust computations, even in the presence of a strong shock or volume fraction discontinuity. This marked the first achievement of the standalone AUSM-family schemes. Nevertheless, AUSM$^+$-upf inherited tunable parameters from AUSM$^+$-up (with several additional parameters) without any explicit physical explanations, which require careful tuning by the user depending on each problem.

On the other hand, in the field of gas dynamics simulation, Shima [12] proposed a SLAU (Simple Low-dissipation AUSM) scheme, which is an improved AUSM-family scheme capable of performing stable and high-resolution calculations corresponding from low to high Mach numbers. SLAU is simpler than the existing all-speed AUSM family schemes and does not involve any tunable parameters. As a result, it can be easily coded and extended to complex physical interactions, such as multi-species and multiphase flows. Its supersonic characteristics were further improved by SD (Shock-Detecting)-SLAU proposed by Shima [13] and SLAU2 proposed by Kitamura [14]. Kitamura [15] demonstrated that a reduction in numerical dissipation reduces numerical errors and enables the calculation of high-resolution results. In recent years, SLAU and SLAU2 have been applied to aerodynamic problems [16,17] and combustion flows in [18]. In addition, the original SLAU2 scheme has already been extended to multiphase flows in combination with the Godunov solver, as mentioned previously [6]. In this context, inspired by AUSM$^+$-upf, we introduce an appropriate amount of dissipation into SLAU2 to execute analogues of the carbuncle-suppression mechanism in gas dynamics interactions, e.g., multiphase flows expressed by the 6-equation model, and verify the robustness and stability of the solutions using several benchmark problems [19].

2. Numerical methods

2.1. Two-fluid modeling (or effective-fluid modeling, EFM)

In this section, the original two-fluid solver proposed in [3,19,6] is first briefly presented using a gas-liquid system as an example. Henceforth, a gas-liquid system is considered in the present study, unless otherwise mentioned. The two-dimensional compressible Euler equations used in two-fluid modeling (or effective fluid modeling, EFM) are as follows:

$$\frac{\partial \boldsymbol{Q}_k}{\partial t}+\frac{\partial \boldsymbol{E}_k}{\partial x}+\frac{\partial \boldsymbol{F}_k}{\partial y}=\boldsymbol{P}_k^{int}+\boldsymbol{S}_k, k=g,l \tag{1}$$

$$\boldsymbol{Q}_k=\begin{bmatrix}\alpha\rho\\ \alpha\rho u\\ \alpha\rho v\\ \alpha\rho E\end{bmatrix}_k,\ \boldsymbol{E}_k=\begin{bmatrix}\alpha\rho u\\ \alpha\left(\rho u^2+p\right)\\ \alpha\rho vu\\ \alpha\rho uH\end{bmatrix}_k,\ \boldsymbol{F}_k=\begin{bmatrix}\alpha\rho v\\ \alpha\rho uv\\ \alpha\left(\rho v^2+p\right)\\ \alpha\rho vH\end{bmatrix}_k,$$

$$\boldsymbol{p}^{int}=\begin{bmatrix}0\\ p^{int}\frac{\partial\alpha}{\partial x}\\ p^{int}\frac{\partial\alpha}{\partial y}\\ -p^{int}\frac{\partial\alpha}{\partial t}\end{bmatrix}_k,\ \boldsymbol{S}_k=\begin{bmatrix}0\\ \alpha\rho g_x\\ \alpha\rho g_y\\ \alpha\rho g_x u+\alpha\rho g_y v\end{bmatrix}_k \tag{2}$$

$$\alpha_g+\alpha_l=1 \tag{3}$$

$$p_g=p_l\equiv p \tag{4}$$

$$p_g^{int}=p_l^{int}\equiv p^{int} \tag{5}$$

$$p^{int}=p-\delta p^* \tag{6}$$

where α denotes the volume fraction of a fluid, ρ denotes the density, u and v denote the velocity components in the Cartesian coordinates, E denotes the total energy per unit mass [$E=e+(p/\rho)$], where e denotes the internal energy], p denotes the pressure, H denotes the total enthalpy [$H=E+(p/\rho)$], and g_x and g_y denote the $x-$ and $y-$components of the gravity vector (of magnitude 9.8 m/s^2). $k=g,l$ represent the gas and liquid, respectively. As in the notation of the single fluid equation, $\boldsymbol{Q}_k$ denotes the conservative vector, and $\boldsymbol{E}_k$ and $\boldsymbol{F}_k$ denote the inviscid flux vectors in the $x-$ and $y-$directions, respectively, but they include α. Additionally, the interfacial pressure, p^{int}, proposed by Stuhmiller [4], and the source term containing the gravity force, $\boldsymbol{S}_k$, considered in the context of the "Faucet problem" proposed by Ransom [20], are also included in the formulation in this study. Eq. (3) expresses the compatibility relation for the volume fractions, Eq. (4) and Eq. (5) assumes a pressure equilibrium, and Eq. (6) yields the interface pressure, p^{int}, which deviates from p by δp^*, which will be explained later. In addition, we adopted the stiffened-gas model proposed by Harlow [21] as an equation of state (EOS) for closing the system.

$$p_k = \rho_k \frac{\gamma_k - 1}{\gamma_k} C_{pk} T_k - p_{k\infty} \tag{7}$$

$$e_k = \frac{C_{pk}}{\gamma_k} T_k + \frac{p_{k\infty}}{\rho_k} \tag{8}$$

where e_k denotes the internal energy per unit mass of fluid, k. a_k denotes the speed of sound as follows:

$$a_k = \left(\gamma_k \left(\frac{p_k + p_{k\infty}}{\rho_k} \right) \right)^{1/2} \tag{9}$$

$$\gamma_g = 1.4,\ C_{pg} = 1004.5\ [\mathrm{J/(kg \cdot K)}],\ p_{g_\infty} = 0\ [\mathrm{Pa}] \quad \textit{for air} \tag{10a}$$

$$\gamma_l = 2.8,\ C_{pl} = 4186.0\ [\mathrm{J/(kg \cdot K)}],\ p_{l_\infty} = 8.5 \times 10^8\ [\mathrm{Pa}] \quad \textit{for water} \tag{10b}$$

The gas and liquid were taken to be air and water, respectively. The physical property values in the stiffened gas model are expressed by Eq. (10). The ideal gas law is treated as a special case of a stiffened gas EOS. Finally, we have 14 unknowns $\left(\alpha,\ \rho,\ u,\ v,\ e,\ p,\ p^{int}\right)_{g,l}$ related by 12 equations with two EOSs. The feature of Eq. (1), the interface pressure, p^{int}, is applied to the cell at the gas-liquid interface. Here, δp^* of a gas-liquid system is usually given by the following:

$$\delta p^* = \sigma \frac{\alpha_g \alpha_l \rho_g \rho_l}{\alpha_g \rho_l + \alpha_l \rho_g} \left| \boldsymbol{u}_l - \boldsymbol{u}_g \right|^2 \tag{11}$$

The interfacial pressure coefficient, σ, must be sufficiently large to maintain the hyperbolic system. In this study, Eq. (11) with $\sigma = 2.0$ [19] is adopted. Further, to prevent p^{int} from becoming excessively low, the following limitation is imposed.

$$\delta p^* = \min(\delta p^*, \varepsilon_p p) \tag{12}$$

where $\varepsilon_p = 0.01$ [19] was used, as in the reference for all numerical experiments.

2.2. Effective fluid model and spatial discretization

This solver is based on the concept of the stratified flow model initially proposed by Stewart [22] and later refined by Liou [3]. The interfacial pressure, p^{int}, is required to operate within the volume fraction discontinuities without switching to the exact Riemann solver. Even though the volume fractions exhibit discontinuities at the cell interfaces, they are continuous within the cell. As an illustrative example, the one-dimensional discretized form of Eq. (1), calculated via the finite volume method, is given by the following:

$$\frac{Vol_j}{\Delta t} \Delta \boldsymbol{Q}_j + \boldsymbol{E}_{j+1/2} S_{j+1/2} - \boldsymbol{E}_{j-1/2} S_{j-1/2} = p^{int} \begin{bmatrix} 0 \\ \alpha_{j+1/2,L} - \alpha_{j-1/2,R} \\ \frac{Vol_j \left(\alpha_j^{n+1} - \alpha_j^n \right)}{\Delta t} \end{bmatrix} + \boldsymbol{S}_j \tag{13}$$

where the phase-subscript k is omitted, j denotes the cell index, Vol_j denotes the volume of the cell. All cell-interface variables, $\phi_{j+1/2,L/R}$, were calculated via spatially second-order accurate MUSCL interpolation proposed by van Leer [23] with van Albada's limiter [24]. In this work, the explicit 3-stage third-order TVD Runge–Kutta (RK3) scheme is used [25]. Other aspects of the computational method are described in [6].

2.3. SLAU2 flux and its modification

An AUSM-family numerical flux, AUSM$^+$-up, AUSM$^+$-upf, or SLAU2, is used to calculate inviscid numerical fluxes at cell interfaces corresponding to each phase, denoted by $\boldsymbol{F}_{k,1/2,L/R}$ where L and R indicated left and right cells, respectively. The AUSM-family numerical fluxes for multiphase flows are expressed as follows:

$$\boldsymbol{F}_{k,1/2,L/R} = \frac{\dot{m}_{1/2,k} + \left| \dot{m}_{1/2,k} \right|}{2} \boldsymbol{\Psi}_{k,L} + \frac{\dot{m}_{1/2,k} - \left| \dot{m}_{1/2,k} \right|}{2} \boldsymbol{\Psi}_{k,R} + \alpha_{k,1/2,L/R} \tilde{p}_{k,1/2} \boldsymbol{N} \tag{14}$$

$$\boldsymbol{\Psi}_k = (\alpha, \alpha u, \alpha v, \alpha H)_k^T,\ \boldsymbol{N} = \left(0, n_x, n_y, 0\right)^T \tag{15}$$

where n_x and n_y denote the $x-$ and $y-$normal components, respectively, to the cell interfaces.

In this subsection, we introduce SLAU2 for multiphase flows, as proposed by Kitamura [6]. The mass flux for each fluid is expressed as follows:

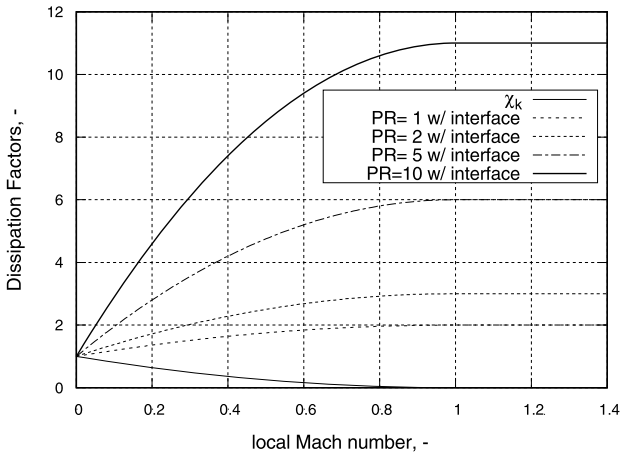

Fig. 1. Comparison of dominant dissipation factors at different pressure ratios at the gas-liquid interface.

$$\left(\dot{m}_{k,1/2}\right)_{SLAU2} = \frac{1}{2}\left\{\rho_{k,L}\left(V_{k,nL} + \left|\overline{V}_{k,n}\right|^{+}\right) + \rho_{k,R}\left(V_{k,nR} - \left|\overline{V}_{k,n}\right|^{-}\right) - \chi_k/a_{1/2,k}(p_R - p_L)\right\} \tag{16}$$

$$\left|\overline{V}_{k,n}\right|^{+} = (1-g_k)\left|\overline{V}_{k,n}\right| + g_k\left|V_{k,nL}\right|,\ \left|\overline{V}_{k,n}\right|^{-} = (1-g_k)\left|\overline{V}_{k,n}\right| + g_k\left|V_{k,nR}\right| \tag{17}$$

$$\left|\overline{V}_{k,n}\right| = \frac{\rho_{k,L}\left|V_{k,nL}\right| + \rho_{k,R}\left|V_{k,nR}\right|}{\rho_{k,L} + \rho_{k,R}} \tag{18}$$

$$g_k = -\max\left[\min\left(M_{k,L}, 0\right), -1\right] \cdot \min\left[\max\left(M_{k,R}, 0\right), 1\right] \in [0, 1] \tag{19}$$

$$\chi_k = \left(1 - \hat{M}_k\right)^2 \tag{20}$$

$$\hat{M}_k = \min\left(1.0, \frac{1}{a_{1/2}}\sqrt{\frac{\boldsymbol{u}_{k,L}^2 + \boldsymbol{u}_{k,R}^2}{2}}\right) \tag{21}$$

$$M_k = \frac{V_{k,n}}{a_{1/2}} = \frac{u_k n_x + v_k n_y}{a_{1/2}} \tag{22}$$

Further, the pressure flux is given by the following.

$$\begin{aligned}\left(\tilde{p}_{k,1/2}\right)_{SLAU2} = {} & \frac{p_L + p_R}{2} + \frac{P_{(5)k}^{+}\left(M_{k,L}\right)\Big|_{\alpha_s=0} - P_{(5)k}^{-}\left(M_{k,R}\right)\Big|_{\alpha_s=0}}{2}\left(p_L - p_R\right) \\ & + \frac{\sqrt{\boldsymbol{u}_{L,k}^2 + \boldsymbol{u}_{R,k}^2}}{2}\left(P_{(5)k}^{+}\left(M_{k,L}\right)\Big|_{\alpha_s=0} + P_{(5)k}^{-}\left(M_{k,L}\right)\Big|_{\alpha_s=0} - 1\right)\overline{\rho}a_{1/2,k}\end{aligned} \tag{23}$$

$$P_{(5)}^{\pm}\left(M_k\right)|_{\alpha_s} = \begin{cases} \frac{1}{2}\left(1 \pm sign\left(M_k\right)\right), & if\ |M| \geq 1 \\ \frac{1}{4}\left(M_k \pm 1\right)^2\left(2 \mp M_k\right) \pm \alpha_s M\_k\left(M_k^2 - 1\right)^2, & otherwise \end{cases} \tag{24}$$

Jack [26] investigated the importance of using appropriate speeds of sound in numerical fluxes. The pressure flux term in Eq. (23), and the final term in Eq. (23) are numerical dissipation terms for low-speed capability and carbuncle suppression in gas dynamics, but their appropriate values for gas-liquid interfaces are yet to be rigorously derived.

2.3.1. Mass flux modification

The value of dissipation for the SLAU2 mass flux, represented by the third term in Eq. (16), was designed to decrease with an increase in the local Mach number and be inoperational when the local Mach number is supersonic or hypersonic. In Fig. 1, the dominant dissipation factor for the SLAU2 mass flux based on the local Mach number is denoted by χ. Because the dissipation term (the third term in Eq. (16)) is inoperational at supersonic speeds, it is evident that oscillations occur behind oblique shock waves [13]. Further, Kitamura [6] observed that the SLAU2 scheme without the exact Riemann (Godunov) solver induces negative pressure in regions where strong shocks coexist with gas-liquid interfaces in multiphase flows. In particular, the Shock/Air-Bubble interaction problem makes the calculation unstable immediately after the incidence of the water shock on the air bubble (this will be further discussed in Section 3.3).

Let us now consider the AUSM$^+$-upf flux scheme. The mass flux dissipation term in AUSM$^+$-upf is also operational in the supersonic regime, as in the case of SLAU2. On the other hand, AUSM$^+$-upf is designed to add a certain amount of dissipation at the gas-liquid interface by adding a new term to the mass flux.

Therefore, in the supersonic regime, we consider an appropriate amount of dissipation for SLAU2 at the gas-liquid interface. In this paper, *we propose the amount of dissipation for mass flux in accordance with the strength of shock waves at the gas-liquid interface* in Eq. (25). In practice, the amount of dissipation is corrected only when the volume fraction discontinuity (depicted in Fig. 1) or the effective length expressed in Eq. (26) is larger than a prescribed threshold [19], and when the shockwave is expected to interact with the phase discontinuity [Note: χ_k is zero at a supersonic speed (= upstream of the shockwave), according to Eqs. (20)–(21), but unity in a subsonic regime, leading to an unaltered equation from the last term of Eq. (16)].

$$\begin{cases} \left(\frac{\max(p_L,p_R)}{\min(p_L,p_R)}(1-\chi_k)+1\right)\frac{p_L-p_R}{a_{1/2,k}} & \text{if } \Delta_{eff} > 5\varepsilon \\ \chi_k \frac{p_L-p_R}{a_{1/2,k}} & \text{otherwise} \end{cases} \tag{25}$$

$$\Delta_{eff} = \mid \alpha_{g,1/2,L} - \alpha_{g,1/2,R} \mid \tag{26}$$

where ε denotes a small number corresponding to each problem, whose effect is examined in Section 3.2. The dissipation factor at the gas-liquid interface is denoted by "PR=1 w/ interface" when the pressure ratios of both the left and right cells are unity, as depicted in Fig. 1. The PR in Fig. 1 denotes the pressure ratio, $\frac{\max(p_L,p_R)}{\min(p_L,p_R)}$. Similarly, "PR=2, 5 and 10 w/ interface" in Fig. 1 expresses that the pressure ratio between the left and right cells at the gas-liquid interface is 2, 5, and 10, respectively. Even if a shock wave is incident on the gas-liquid interface, SLAU2 with dissipation defined by Eq. (25) is expected to be able to obtain stable solutions without using the exact Riemann (Godunov) solver.

2.3.2. Pressure flux modification

Numerical instability is known to occur even in the water-to-air shock tube problem with a high-pressure ratio, as discussed in [6]. It has been observed that the numerical flux of the AUSM family leads to a negative pressure flux in regions where strong shocks coexist with volume fraction discontinuities. This negative pressure is considered to be caused by the dissipation term in the third term of Eq. (23). This pressure-velocity coupling term is too large in the case of multiphase flow owing to the high speed of sound [10]. Therefore, we considered an appropriate numerical dissipation term for the pressure flux. In this study, as proposed in Eq. (27), the pressure flux dissipation at the gas-liquid interface, originally expressed by the third term in Eq. (23), is calculated based on the difference in the velocity between the gas and liquid phases. We examined the required amount of numerical dissipation at the volume fraction discontinuities to produce the effect of the proposed dissipation term in Section 3.2.

$$\begin{cases} \lambda_{mr}\left(P^+_{(5)}\left(M_{k,L}\right)\mid_{\alpha_s}=0 + P^-_{(5)}\left(M_{k,R}\right)\mid_{\alpha_s=0} - 1\right)\overline{\rho}a_{1/2} & \text{if } \Delta_{eff} > 5\varepsilon \\ \frac{\sqrt{u^2_{k,L}+v^2_{k,R}}}{2}\left(P^+_{(5)}\left(M_{k,L}\right)\mid_{\alpha_s=0} + P^-_{(5)}\left(M_{k,R}\right)\mid_{\alpha_s=0} - 1\right)\overline{\rho}a_{1/2} & \text{otherwise} \end{cases} \tag{27}$$

$$\lambda_{mr} = \left|\sqrt{(\boldsymbol{u}^2_{g,L}+\boldsymbol{u}^2_{g,R})/2} - \sqrt{(\boldsymbol{u}^2_{l,L}+\boldsymbol{u}^2_{l,R})/2}\right| \tag{28}$$

Eq. (27) uses multidimensional velocity instead of normal velocity. This idea was inherited from SLAU and SLAU2, which were used to successfully eliminate the need for tunable parameters (cutoff Mach number) in [12].

3. Numerical experiments

The numerical results obtained via the selected flux schemes and the proposed flux scheme for benchmark problems are compared in this subsection. The original SLAU2, AUSM$^+$-upf, and the modified SLAU2 proposed in this study (in the graph, it has been denoted by "Modified SLAU2") are considered. The dissipation tunable parameters used for AUSM$^+$-upf are taken to be $\left(K_u, K_p\right) = (1, 1)$.

3.1. Ransom's Faucet problem

This problem is the well-known "Faucet problem" proposed by Ransom [20], in which a water jet is injected into stationary air at a speed of 10 m/s and is accelerated downward by gravity in a 12 m long tube. In this problem, the gravity term in Eq. (1) was applied. This is typically modeled using the following initial conditions:

$$\left(p, \alpha_g, u_g, u_l, T_g, T_l\right) = (10^5 \text{ Pa}, 0.2, 0 \text{ m/s}, \ 10 \text{ m/s}, 300 \text{ K}, 300 \text{ K}) \tag{29}$$

The tow-fluid model is capable of considering the gas liquid velocity corresponding to each phase separately.

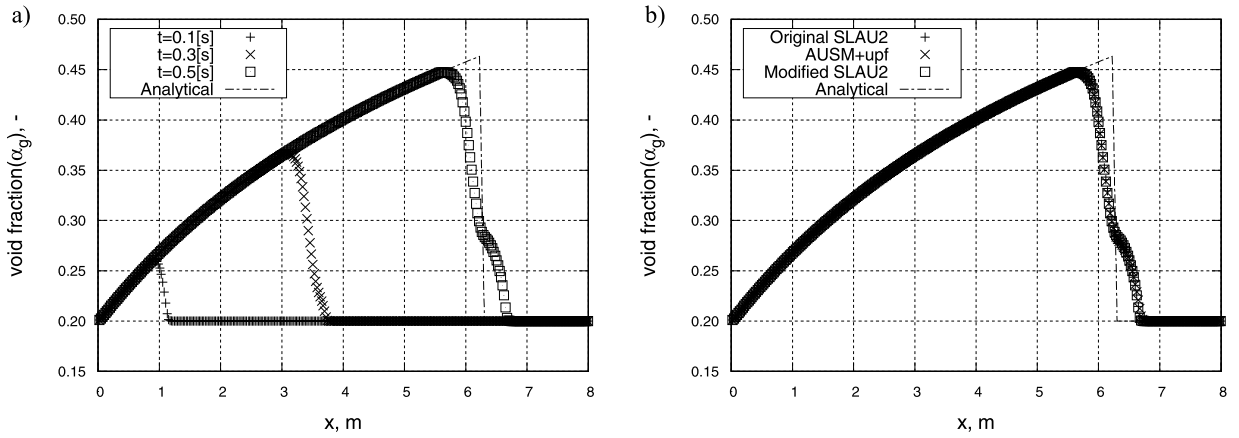

Fig. 2. a) Volume fractions of gas phase for the Faucet problem of Modified SLAU2 at $t = 0.1$ s, 0.3 s, and 0.5 s, with exact solution at $t = 0.5$ s. b) Faucet problem solutions for 3 schemes at $t = 0.5$ s.

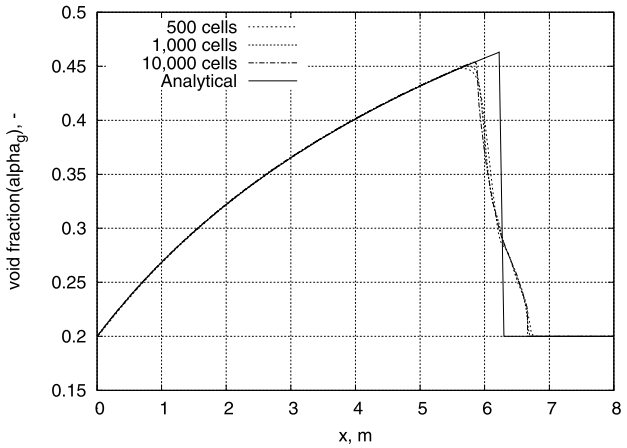

Fig. 3. Grid convergence with a smooth profile in the case of the Faucet problem.

Here, 500 uniform cells were used for the domain [0 m, 12 m]. The computed results were compared with the analytical solution obtained by Paillére [27]:

The volume fractions at $t = 0.1$ s, 0.3 s, and 0.5 s have been depicted in Fig. 2a. The propagation of the volume-fraction wave was accurately computed. Additionally, the volume fraction profiles at $t = 0.5$ s have been depicted in Fig. 2b. The results of all schemes were observed to be in good agreement with each other.

Further, to verify the influence of the grid, the problem was solved using three different grids.

- 500 cells : $\Delta x = 0.024$ m
- 1,000 cells : $\Delta x = 0.012$ m (30)
- 10,000 cells : $\Delta x = 0.0012$ m

As depicted in Fig. 3, grid convergence was realized with a smooth profile. As the number of grid points was increased, the numerical solution was observed to converge.

3.2. Water-to-air shock tube with high pressure ratio, PR=1,000

As mentioned by Kitamura [6], this high-pressure-ratio water-to-air shock tube problem cannot be solved using the AUSM-family fluxes without using the exact Riemann solver. In Sections 3.2–3.3, $\varepsilon = 1.0 \times 10^{-7}$ was adopted. However, in previous studies on this benchmark problem, $\varepsilon = 1.0 \times 10^{-5}$ was adopted [19]. Therefore, we also investigated the effect of ε on the benchmark problem. This test represents a one-dimensional test case with the following initial conditions:

$$\left(p, \alpha_g, u_k, T_k\right) = \left(10^8 \text{ Pa}, \varepsilon, 0 \text{ m/s}, 308.15 \text{ K}\right) \quad \textit{for } x \leq 5 \text{ m} \tag{31}$$

$$\left(p, \alpha_g, u_k, T_k\right) = \left(10^5 \text{ Pa}, 1-\varepsilon, 0 \text{ m/s}, 308.15 \text{ K}\right) \quad \textit{for } x > 5 \text{ m} \tag{32}$$

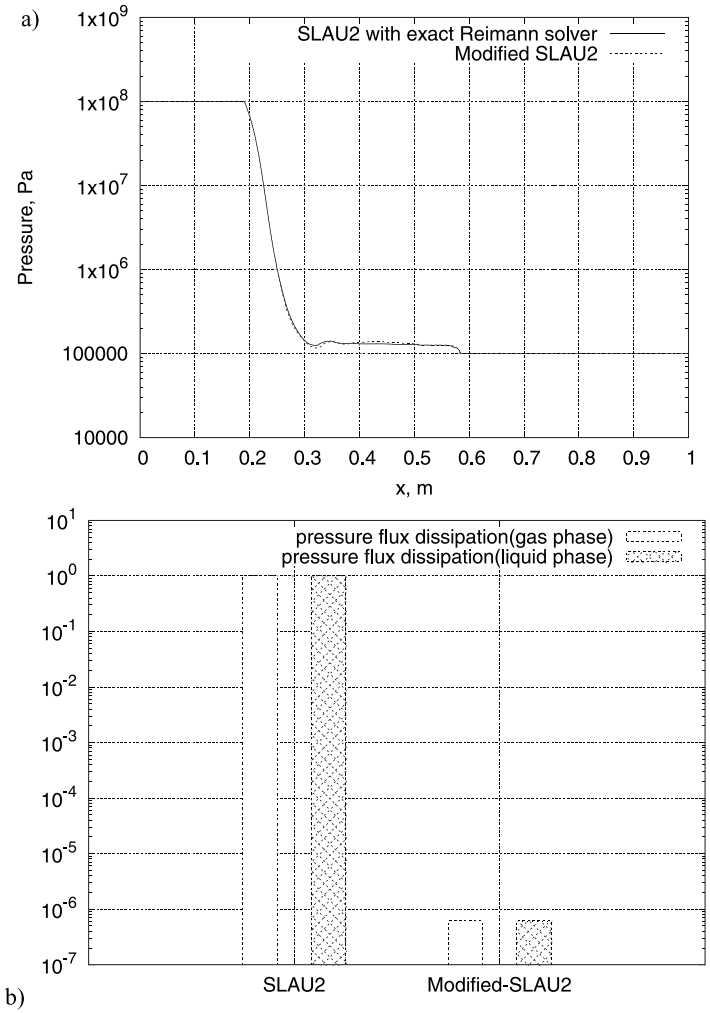

Fig. 4. a) Results obtained via Modified SLAU2 and SLAU2 with exact Riemann solver for the Water-to-air shock tube problem with a high pressure ratio at $t = 2$ ms. b) Comparison of the amounts of numerical dissipation at $t = 2$ ms (normalized by the original SLAU2 value).

where $k = g, l$. The results exhibited good correspondence with the references cited in [6]. The proposed modifications to the SLAU2 fluxes allowed this high-pressure-ratio shock tube problem to be solved without the exact Riemann solver, as illustrated in Fig. 4a.

Subsequently, we attempted to estimate the dissipation term for the proposed pressure flux. For this purpose, owing to the divergence of the numerical calculation using the (original) SLAU2 at $t \approx 35$ μs, we restarted the SLAU2 computation by using the flow field after 2 ms of computation using the modified SLAU2. Then, the amounts of dissipation of the original SLAU2 and modified SLAU2 were compared at the void fraction discontinuities. In this shock tube problem, the velocity was generated at the void fraction discontinuities owing to the pressure difference. In the original SLAU2, the numerical dissipation was determined by the product of velocity and the speed of sound, which induced an excessive numerical dissipation at the interface between the gas and liquid phases, resulting in negative pressure (Fig. 4b). In contrast, in the modified SLAU2, the numerical dissipation was determined by the relative velocity. Owing to its low value at the void fraction discontinuities, a stable calculation was realized using the proposed numerical dissipation. Further, because of the absence of any pressure difference at the gas-liquid interface after 2 ms, the dissipation of the mass flux was not applicable.

In addition, the modified SLAU2 was observed to be approximately 13 times faster than the exact Riemann solver while calculating the flux at the interface between the gas and liquid. The calculations were conducted using an Intel$^{(R)}$ Core$^{(TM)}$ i5-6360U CPU@2.00GHz.

Moreover, in the literature (e.g., [6,10,29]), the pressure distributions (particularly in the expansion fan) were found to depend significantly on the value of ε, as depicted in Fig. 5. Nevertheless, we obtained reasonable results with $\varepsilon = 1.0 \times 10^{-7}$, and achieved convergence with respect to ε (i.e., the solution was insensitive to the value below 1.0×10^{-7}). Therefore, we chose $\varepsilon = 1.0 \times 10^{-7}$ in this paper.

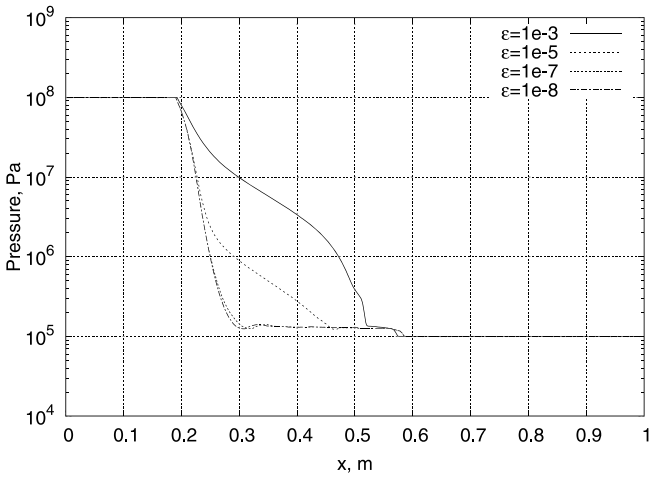

Fig. 5. Water-to-air shock tube problem with high pressure ratio (PR = 1,000) solutions with different ϵ at $t = 2$ ms.

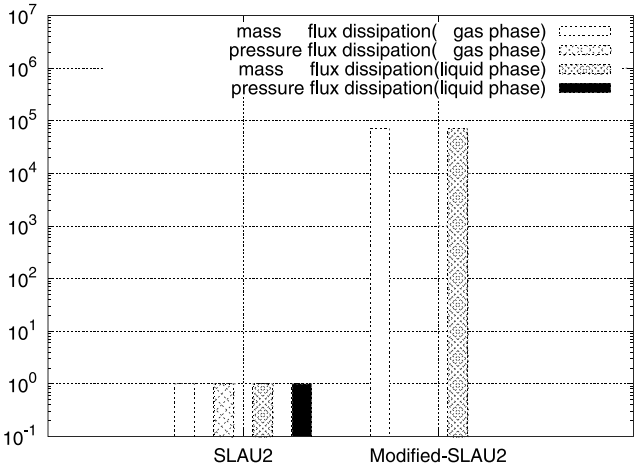

Fig. 6. Comparison of the amounts of numerical dissipation at the time of incidence of the water shock on the bubble (normalized by the original SLAU2 value) at $x = -3.2$ mm, $y = 0$ mm at $t \approx 0.3$ μs.

3.3. 2D shock/air-bubble interaction

This problem considers the incidence of a water shock on an air bubble, with a much higher pressure ratio (PR = 1.6×10^4). The initial conditions were identical to those presented in [19]. $1{,}400 \times 600$ isotropic cells were used corresponding to the domain, $[-15$ mm, 20 mm$] \times [0$ mm, 15 mm$]$, to cover the 6.4 mm diameter water column with its center at the origin (i.e., the diameter was 256 times the grid spacing, $\Delta x_{\min} = \Delta y_{\min} = 0.025$ mm).

$$\begin{aligned} &(p, \alpha_g, u_k, T_k) = \left(1.6 \times 10^9 \text{ Pa}, 1-\varepsilon, 661.81 \text{ m/s}, 595.13 \text{ K}\right) \quad \textit{for } x \le -4 \text{ mm} \\ &(p, \alpha_g, u_k, T_k) = \left(1.01325 \times 10^5 \text{ Pa}, 1-\varepsilon, 0 \text{ m/s}, 293.15 \text{ K}\right) \quad \textit{for } x > -4 \text{ mm} \\ &\quad \textit{except for } x^2 + y^2 < 3.2^2 \text{ mm}^2 \quad \textit{where } \alpha_g = \varepsilon \end{aligned} \tag{33}$$

Then, the shock was displaced with $M_{sh} = 1.51$, and became incident on the air bubble at $t \approx 0.3$ μs. As mentioned in a previous study [6], in the absence of the exact Riemann (Godunov) solver, the AUSM-family fluxes diverged as soon as the shock was incident on the bubble.

Let us compare the amount of numerical dissipation of mass and pressure flux at this location ($x = -3.2$ mm, $y = 0$ mm) corresponding to SLAU2 and Modified SLAU2 (right before the divergence of SLAU2 at $t \approx 0.3$ μs). The amount of mass flux dissipation in the case of Modified SLAU2 was approximately 70,000 times larger than that in SLAU2 (Fig. 6) as per the design described in Section 2.3.1. As the shock is incident on the bubble, the flow condition becomes close to the supersonic region and the pressure ratio was observed to be high at this location). On the other hand, the pressure flux dissipation of the modified SLAU2 was not applicable due to the absence of relative velocity.

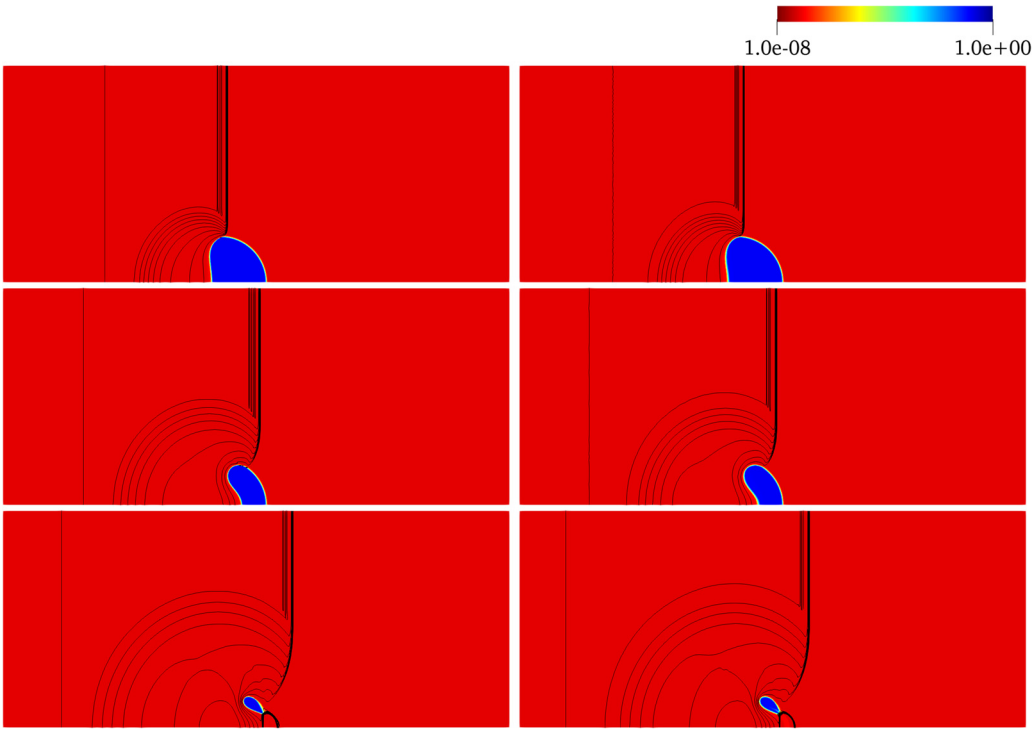

Fig. 7. Results obtained via Modified SLAU2 (left) and SLAU2 with exact Riemann solver (right). Volume fraction contours with pressure contour lines for shock/air-bubble interaction problem at $t = 2$ μs (top), 3 μs (middle), and 4 μs (bottom).

The modified SLAU2 was verified to be capable of computing this challenging problem, as depicted in Fig. 7 and 8, by using the numerical Schlieren function, $\log(|\nabla\rho| + 1)$. The contours exhibited good agreement with the references cited in [6] and [28]. We also compared the results obtained via the proposed SLAU2 scheme and "SLAU2 with exact Reimann solver," which is considered to be a stable and accurate method. The comparison is presented in Fig. 8. The deformations of the air bubble and the pressure distributions obtained via the two methods were observed to be very similar.

These results demonstrate that the proposed SLAU2 equipped with a modified, proper dissipation term is capable of handling such challenging problems without using the exact Riemann solver, which is expensive and susceptible to the carbuncle phenomenon.

4. Conclusions

In this paper, we proposed a modified SLAU2 numerical flux scheme without tunable parameters for compressible multiphase flows, which exhibits low dissipation, yet is stable. Numerical experiments were conducted to verify that the modified SLAU2 scheme is capable of computing a wide spectrum of multiphase flows without numerical instability or serious oscillations. We concluded that SLAU2 with an appropriate amount of dissipation at the gas-liquid interface can obtain stable solutions even in the presence of a strong shock or a high-pressure ratio. The modifications did not involve any iterative procedures, such as those required by the exact Riemann solver; thus, its computational cost is quite low. The results herein may also serve as crucial factors for the further development of numerical modeling for multiphase flows. Future studies should investigate i) viscous flow extensions, ii) the addition of source terms for cavitation or chemical reactions, and iii) applications to three-dimensional practical cases and unstructured grids.

CRediT authorship contribution statement

Junya Aono: Conceptualization, Data curation, Formal analysis, Investigation, Methodology, Software, Validation, Visualization, Writing – original draft, Writing – review & editing. **Keiichi Kitamura:** Funding acquisition, Investigation, Methodology, Project administration, Resources, Software, Supervision.

Declaration of competing interest

The authors declare that they have no known competing financial interests or personal relationships that could have appeared to influence the work reported in this paper.

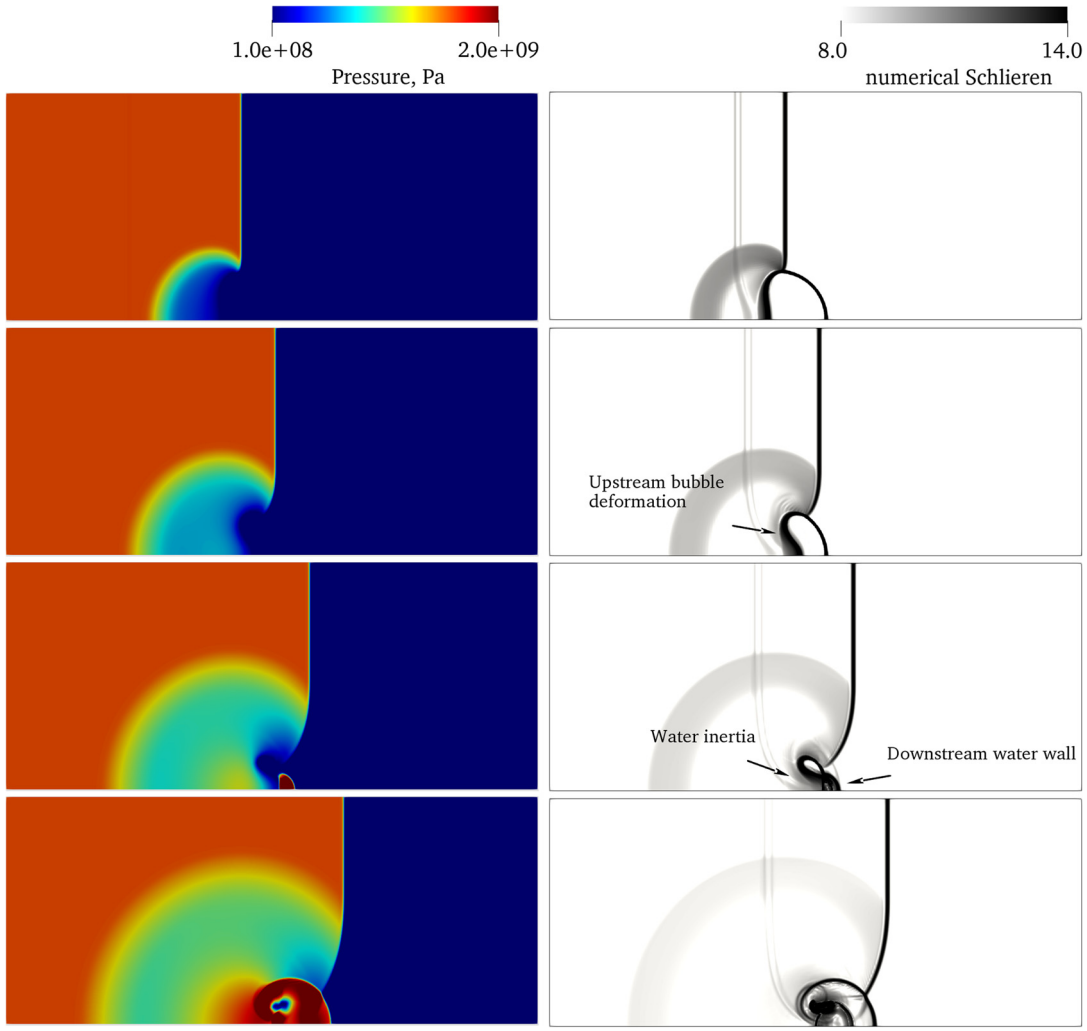

Fig. 8. Pressure (left) and numerical Schlieren (right) contours for shock/air-bubble interaction problem of modified SLAU2 at $t = 2$ μs (top), 3 μs (upper middle), 4 μs (lower middle), and 5 μs (bottom).

Acknowledgements

This work has benefited from discussions with A. K. Pandare at the Los Alamos National Laboratory and H. Luo at North Carolina State University. This work was partly supported by JSPS KAKENHI Grant Number JP19K04834, Grant for Basic Science Research Projects from The Sumitomo Foundation (Grant Number 200159), and Yokohama Academic Foundation. We would like to thank Editage (www.editage.com) for English language editing.

References

[1] H. Tamura, M. Takahashi, M. Sasaki, T. Tomita, W. Mayer, Observation of LOX/hydrogen combustion flame in a rocket chamber during chugging instability, in: 39th AIAA/ASME/SAE/ASEE Joint Propulsion Conference and Exhibit, 2003.
[2] R.W. Houim, E.S. Oran, A multiphase model for compressible granular–gaseous flows: formulation and initial tests, J. Fluid Mech. 789 (2016) 166–220.
[3] M.-S. Liou, C.-H. Chang, L. Nguyen, T.G. Theofanous, How to solve compressible multifluid equations: a simple, robust, and accurate method, AIAA J. 46 (9) (2008) 2345–2356.
[4] J. Stuhmiller, The influence of interfacial pressure forces on the character of two-phase flow model equations, Int. J. Multiph. Flow 3 (6) (1977) 551–560.
[5] S.K. Godunov, Finite difference method for numerical computation of discontinuous solutions of the equations of fluid dynamics, Mat. Sb. 47(89) (3) (1959) 271–306.
[6] K. Kitamura, M.-S. Liou, C.-H. Chang, Extension and comparative study of AUSM-family schemes for compressible multiphase flow simulations, Commun. Comput. Phys. 16 (3) (2014) 632–674.
[7] J.J. Quirk, A contribution to the great Riemann solver debate, Int. J. Numer. Methods Fluids 18 (6) (1994) 555–574.
[8] M.-S. Liou, Mass flux schemes and connection to shock instability, J. Comput. Phys. 160 (2) (2000) 623–648.
[9] Y.-Y. Niu, Y.-C. Lin, C.-H. Chang, A further work on multi-phase two-fluid approach for compressible multi-phase flows, Int. J. Numer. Methods Fluids 58 (8) (2008) 879–896.

[10] A.K. Pandare, H. Luo, A robust and efficient finite volume method for compressible inviscid and viscous two-phase flows, J. Comput. Phys. 371 (2018) 67–91.
[11] M.-S. Liou, A sequel to AUSM, part II: AUSM+-up for all speeds, J. Comput. Phys. 214 (1) (2006) 137–170.
[12] E. Shima, K. Kitamura, Parameter-free simple low-dissipation AUSM- family scheme for all speeds, AIAA J. 49 (8) (2011) 1693–1709.
[13] E. Shima, K. Kitamura, Multidimensional numerical noise from captured shock wave and its cure, AIAA J. 51 (4) (2013) 992–998.
[14] K. Kitamura, E. Shima, Towards shock-stable and accurate hypersonic heating computations: a new pressure flux for AUSM-family schemes, J. Comput. Phys. 245 (2013) 62–83.
[15] K. Kitamura, A. Hashimoto, Reduced dissipation AUSM-family fluxes: HR-SLAU2 and HR-AUSM+-up for high resolution unsteady flow simulations, Comput. Fluids 126 (2016) 41–57.
[16] K. Kitamura, S. Nonaka, K. Kuzuu, J. Aono, K. Fujimoto, E. Shima, Numerical and experimental investigations of epsilon launch vehicle aerodynamics at Mach 1.5, J. Spacecr. Rockets 50 (4) (2013) 896–916.
[17] T. Aogaki, K. Kitamura, S. Nonaka, Numerical study on high angle-of-attack pitching moment characteristics of slender-bodied reusable rocket, J. Spacecr. Rockets 55 (6) (2018) 1476–1489.
[18] M.E. Harvazinski, T. Shimizu, Computational investigation on the effect of the oxidizer inlet temperature on combustion instability, in: AIAA Propulsion and Energy 2019 Forum, 2019.
[19] C.-H. Chang, M.-S. Liou, A robust and accurate approach to computing compressible multiphase flow: stratified flow model and AUSM+-up scheme, J. Comput. Phys. 225 (1) (2007) 840–873.
[20] V. Ransom, Numerical benchmark tests, in: G.F. Hewitt, J.M. Delhay, N. Zuber (Eds.), Multiphase Science and Technology, vol. 3, 1987, pp. 465–467.
[21] F. Harlow, A. Amsden, Fluid Dynamics, Technical Report LA-4700, 1971.
[22] H.B. Stewart, B. Wendroff, Two-phase flow: models and methods, J. Comput. Phys. 56 (3) (1984) 363–409.
[23] B. van Leer, Towards the ultimate conservative difference scheme. V. A second-order sequel to Godunov's method, J. Comput. Phys. 32 (1) (1979) 101–136.
[24] G.D. van Albada, B. van Leer, W.W. Roberts, A Comparative Study of Computational Methods in Cosmic Gas Dynamics, Springer Berlin Heidelberg, Berlin, Heidelberg, 1997, pp. 95–103.
[25] S. Gottlieb, C.-W. Shu, Total variation diminishing Runge-Kutta schemes, Math. Comput. 67 (221) (1998) 73–85.
[26] J. Edwards, Towards unified CFD simulations of real fluid flows, in: 15th AIAA Computational Fluid Dynamics Conference, 2001.
[27] H. Paillére, C. Corre, J.G. Cascales, On the extension of the AUSM+ scheme to compressible two-fluid models, Comput. Fluids 32 (6) (2003) 891–916.
[28] H. Takahira, S. Yuasa, Numerical Simulations of Shock-Bubble Interactions Using an Improved Ghost Fluid Method Volume 1: Symposia, Parts A and B, 2005, pp. 777–785.
[29] A.K. Pandare, H. Luo, J. Bakosi, An enhanced AUSM^{+}-up scheme for high-speed compressible two-phase flows on hybrid grids, Shock Waves 29 (2019) 629–649.